Experimental Technique of Physics
Experimentelle Technik der Physik
Volume 40 (1994), No. 2, 241–257

New optical measuring methods for process analysis and medical technology

Gerhard Wiegleb, Michael Zöchbauer
Hartmann & Braun AG, Development Analyser Technology
Werk Praunheim, Heerstr. 136, 60488 Frankfurt, Germany

Received: 15 September 1994

Abstract. Optical measuring methods have obtained great importance in the application areas process analysis and medical technology. The article describes a few basic approaches where substantial improvements could be achieved in these areas by the development of modern physical technologies. As examples for the process analysis the NIR laser photometer for oxygen determination and the multicomponent FTIR process spectrometer for continuous emission measurement are given. Concerning the medical technology the paper reports about the NDIR photometer for $^{12}CO_2/^{13}CO_2$ measurement and the Fabry-Perot correlation photometer for nitrous oxide determination.

1. Introduction

Optical measuring methods are particularly suitable for highly selective analysis in complex mixtures [1,2]. In particular, the absorption photometers have achieved a sophisticated development level which is being continually enhanced by new physical technologies (e.g. laser technology/microsystem technology). In absorption spectroscopy, the quantum-mechanical transitions between electron, vibration and rotation levels are being used for a selective measurement. The energy difference of such a transition is calculated from:

$$\Delta E = \Delta E_e + \Delta E_v + \Delta E_r. \tag{1}$$

Dependent on the energy difference ΔE, which characterises the wavelength range in the spectrum, one distinguishes between the UV, VIS, IR and microwave spectroscopy. Different measuring methods have established themselves for the various applications (emission control, immission protection, medical technology, motor vehicle exhaust gas test etc.) and they have been optimized with respect to the required detection limit and cross sensitivity. This treatise describes a few basic approaches where substantial improvements could be achieved by the deployment of modern physical technologies.

2. NDIR photometer

For more than fifty years non-dispersive infrared (NDIR) photometers are being used for gas-analytical purposes [3]. A characteristic feature of this technology is the fact that the selectivity is determined by the special design of the detector, rather than by

ISSN 0014-4924 / $ 2.50

a dispersive element (e.g. grating monochromator or dielectric filter). Generally, this type of photometer comprises a broad-band IR radiation source, a cell with a measuring and reference path (N2 filling) and a so-called 2-layer detector [4]. The component to be detected (e.g. CO or NO) is hermetically sealed in the detector. Having absorbed IR radiation in the detector, the energy of the excited molecules is released again by molecular collisions, resulting in slight warming of the enclosed gas. This increase in temperature causes gas expansion. The same effect is produced in the second (rear) chamber, however, in somewhat different spectral regions. Since in accordance with Lambert-Beer law, energy is absorbed primarily from the centre of the absorption line in the first layer, only the marginal regions of the line remain in the second layer. The pressure increase in the 2nd chamber is therefore primarily effected from these marginal zones. The difference in pressure between both chambers is measured with a diaphragm capacitor or microflow sensor. Since the IR radiation is modulated with a chopper, a pressure pulsation corresponding to the modulation frequency is obtained. The ratio between both layers is selected such that the pressure pulsations are somewhat equal in both chambers without preabsorption in the cell. By means of preabsorption in the measuring cell, the radiation is absorbed from the centre, generating a pressure difference which is practically proportional to the gas concentration in the cell. Overlapping of interference components can be optimally compensated with this method, especially when the energy portions from the first and second layers are equal. The optimization can be achieved by changing the layer thickness.

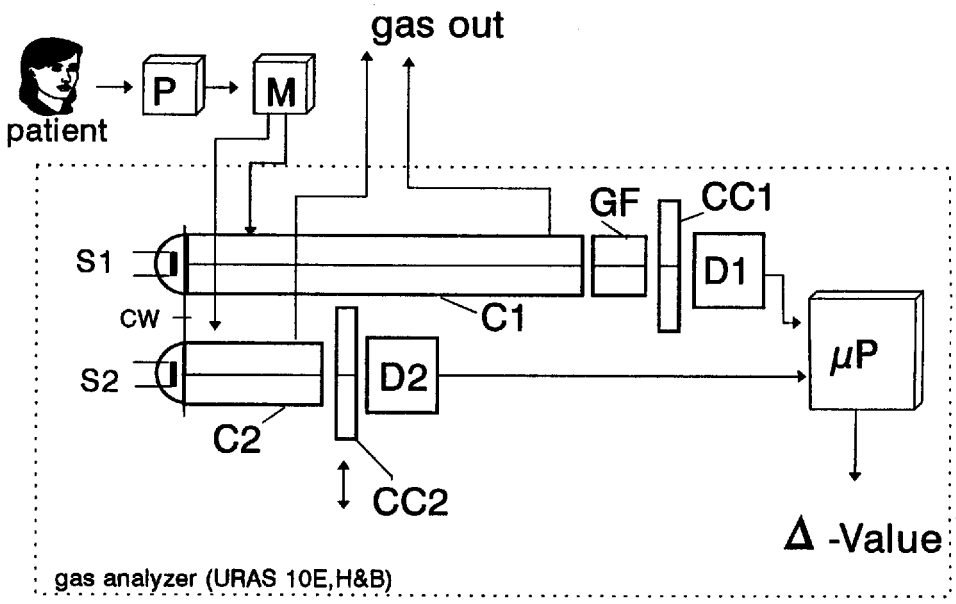

Fig.1. Design of an analyzer for simultaneous determination of $^{13}CO_2$ and $^{12}CO_2$ (P pump, M buffer volume, $S1/S2$ IR radiation source, $C1/C2$ analytic cell, $CC1/CC2$ calibration cell, GF gas filtering cell, $D1/D2$ IR Luft type detector, CW chopper wheel).

The limitations of this method are manifest when various components having similar molecular structure (e.g. different hydrocarbons) must be selectively measured with respect to each other in a single mixture. This is also the case when mixtures of different isotopes (e.g. $^{12}CO_2$ in $^{13}CO_2$) are to be measured. This measurement task is inter alia, in medical technology of paramount importance. Certain metabolic diseases can be detected by means of ^{13}C marked substances (e.g. urea) which are converted into $^{13}CO_2$ during metabolism. The selective measurement of these two isotope compounds in the inhaled air are essential for this diagnosis [5]. Formerly, cumbersome mass spectrometers were deployed for such measurements [6]. Now, this measurement task can be solved with a simple instrument design by means of multicomponent measurement in an NDIR photometer (URAS 10, Hartmann & Braun AG in Frankfurt, Germany). Fig.1 illustrates the optical design of the photometer.

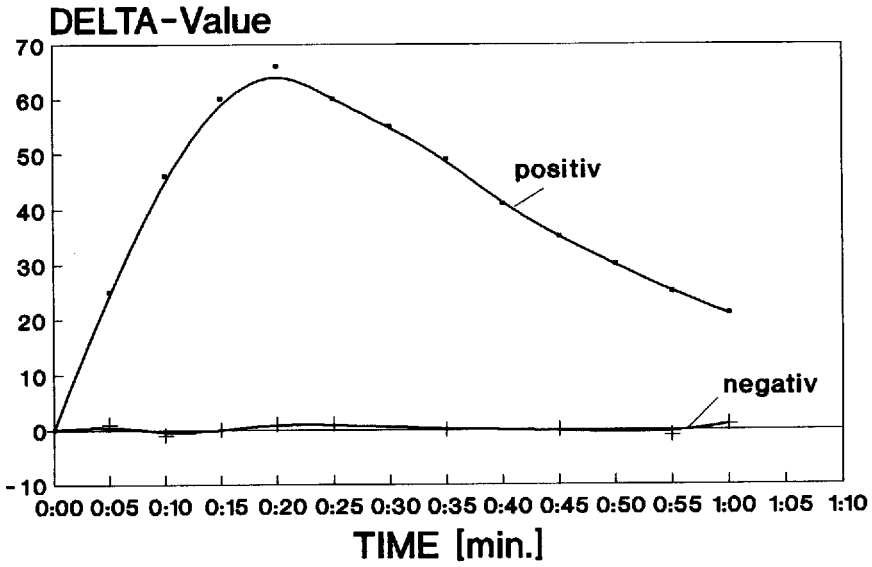

Fig.2. Delta value as a function of the time after administration of ^{13}C marked urea.

The $^{13}CO_2$ measurement is performed in a 200 mm cell since the concentrations are very small. The $^{12}CO_2$ basic level (high concentrations) is acquisitioned in a 20 mm cell in a second optical beam path. The effect of the $^{12}CO_2$ content on the $^{13}CO_2$ measurement is taken into consideration by a computer within the instrument, hence the measured concentrations are without interfering influences whatever they are. The so-called delta value, from which a metabolic illness can be inferred, is determined from the isotope ratio, before and after administering the test substance.
Fig.2 illustrates the measurement results of such a test series. The delta value is calculated here using the following formula:

$$\Delta = 1000 \cdot \frac{(\frac{^{13}CO_2}{^{12}CO_2})_{Meas}}{(\frac{^{13}CO_2}{^{12}CO_2})_{Ref}} - 1. \qquad (2)$$

In the case of a patient without bacterial infection (negative) the delta value does not change after administering a ^{13}C marked urea sample. Conversely, in the case of a positive patient the delta value increases sharply after a few minutes, reaching its maximum peak approximately after 20 minutes. Hence, a simple diagnosis can be made with this analytical method [7] without having to recourse to onerous and unpleasant applications for the patient.

3. NIR laser photometer

Already at an early stage the use of selective radiation sources, in the form of lasers, was reviewed by various teams [8,9]. Apart from the advantages presented by the narrow-band spectral distribution and the practically parallel optical beam path, some disadvantages concerning practical applications came to light too, which to an extent still exist at present. The main ones are:

- high production costs
- short life time
- expensive ancillary optics (e.g. mode selection with monochromator)
- cumbersome supply (e.g. N2 cooling).

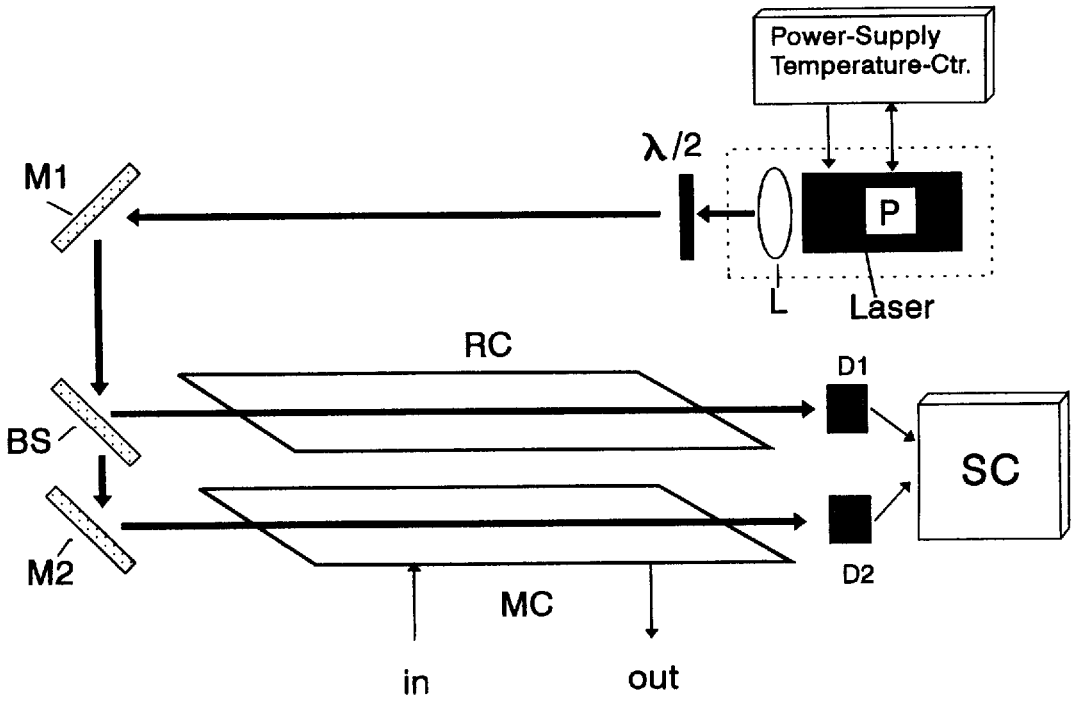

Fig.3. Design of a laser photometer for determination of oxygen (P Peltier cooler, L lens, $M1/M2$ mirror, BS beam splitter, RC reference cell, MC measuring cell, $D1/D2$ solid state detector/Si).

Semiconductor lasers in the VIS/NIR range do not manifest these disadvantages, hence they can be used in analyzers even for process applications. A simple setup for the

spectral region nearby 770 nm is shown in Fig.3. It features essentially a simple semiconductor laser from the communications industry which is cooled with a peltier element to a constant temperature (e.g. 20°C). The polarisation direction of the radiation is predetermined by a $\lambda/2$ plate. After the mirror $M1$, the radiation is divided at the beam splitter BS into two partial beams and falls into a measuring cell MC and reference cell RC. A silicon photodiode is situated behind each cell ($D1, D2$).

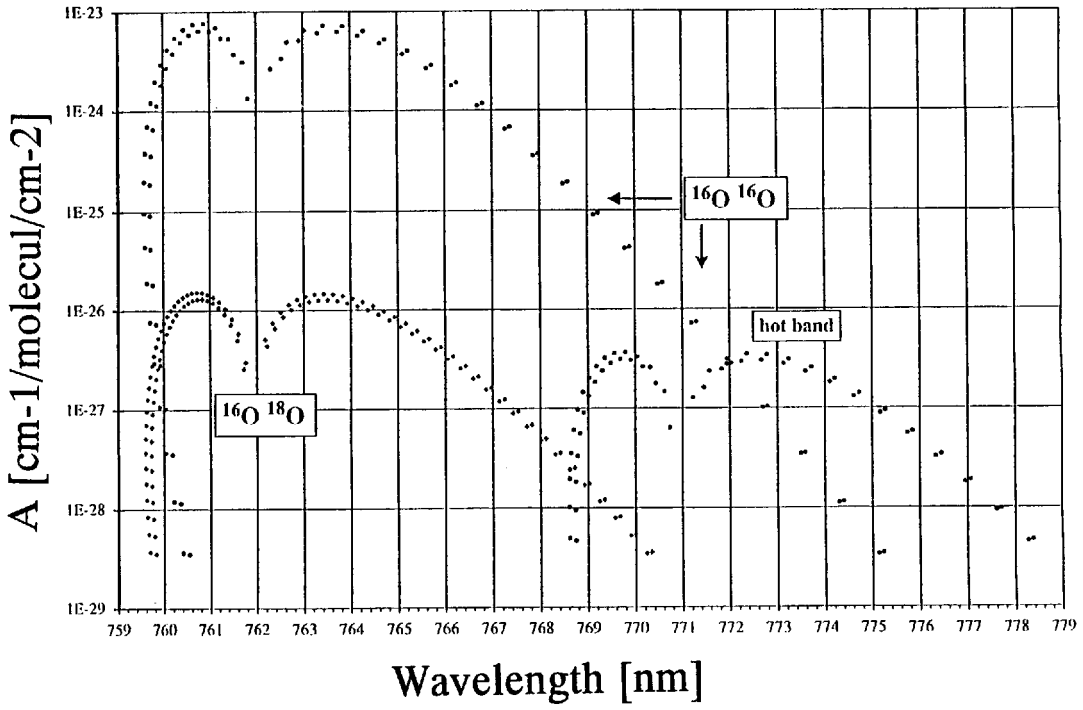

Fig.4. Absorption spectrum of oxygen in the range 760 nm–780 nm.

The input signals are then converted in the processing unit SC into an output signal which is proportional to the concentration of the measured component in the measuring cell. In the spectral region 760 nm–780 nm oxygen features slight absorption bands (see Fig.4) which can be used for a quantitative oxygen determination.

Fig.5 shows an isolated absorption line. The emission wavelength is altered by modulation of the laser diode current so that an intensity distribution is measured according to Fig.5 by diode $D2$ if oxygen is present in the measuring cell. The measured value is calculated in the evaluation electronics SC by computing the individual intensity integrals in the regions of Gate A, B, C. An output signal which is proportional to the concentration is generated by comparison (e.g. quotient formation) with the reference signal ($D1$) [10].

Fig.6 shows the output signal of the evaluation electronics as a function of the time for small oxygen concentrations. The relationship is perfectly linear, hence obviating the

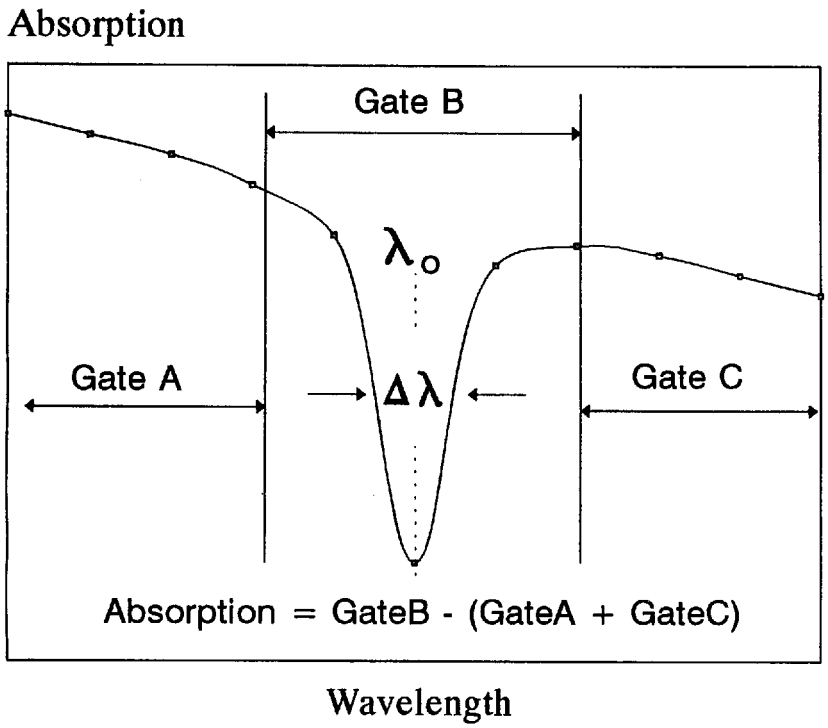

Fig.5. Division of the absorption line into three subregions for determination of the absorption and elimination of interference effects.

need for the linearisation of the output signal. A linear relation can also be presumed for greater concentrations (see Fig.7). This measuring method lends itself particularly to an in-situ setup in order to perform measurements directly in the process or in the stack without cumbersome sampling systems.

4. Fabry-Perot correlation photometer

Apart from the NDIR method described above, there are interferometric correlation procedures based on either the two-beam interference [11] or on the multiple-beam interference [12]. The multiple-beam interference procedure uses a Fabry-Perot interferometer by which the absorption spectrum of the measured component is simulated and "saved" in the measuring instrument. The following text describes a Fabry-Perot correlation photometer [13] which can be used for example for nitrous oxide analysis in medical technology. Its principal component is a newly developed thermally adjustable silicon etalon manufactured in thin-film technology.

Fig.8 illustrates the interferometric principle of the etalon. The etalon consists of a plate P whose front and rear areas are largely plane-parallel to each other. Normally, the areas have dielectric mirrors, transmitting part of the light. Having penetrated the first mirror layer, a beam originating from the light source is frequently reflected to and fro, with a fraction of the energy being expelled towards the back each time. The beams

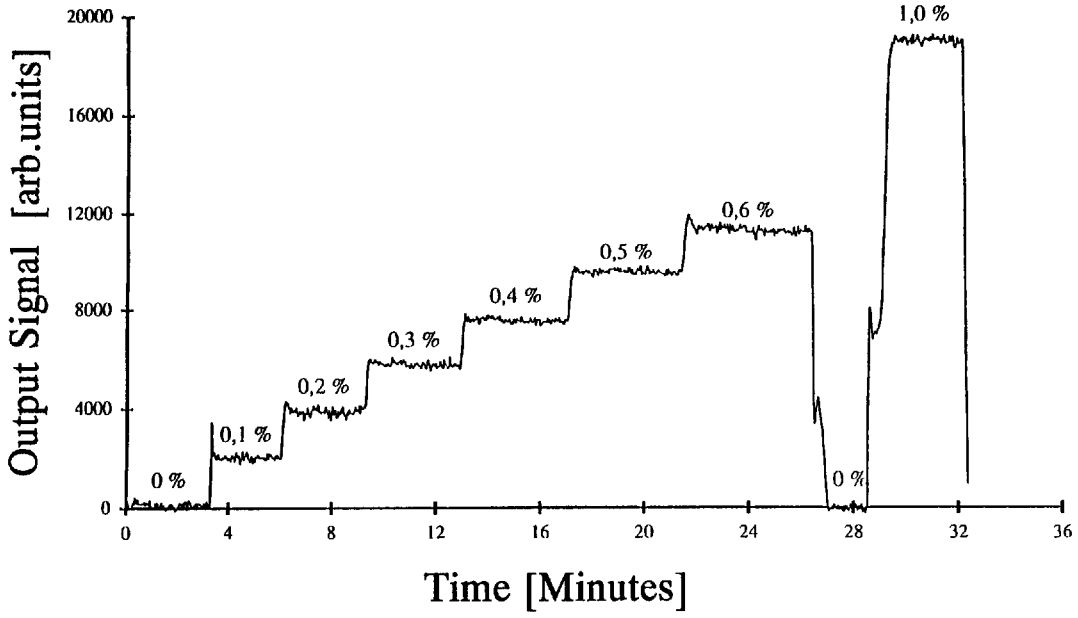

Fig.6. Output signal for diverse oxygen concentrations in nitrogen.

issuing forth from the second mirror layer interfere with each other and are combined in the focal plane of a lense L.

The silicon plate P manufactured in thin film technology has the dimensions 11×11 mm^2 (see Fig.9) and has a surface resistance of $1\ldots10$ Ω·cm. Depending on the measurement task, the thickness of the plate is selected such that the distance between the interference lines is equal to the distance between the rotational lines. The electrodes $E1$ and $E2$ are electrically connected with the silicon plate and serve to apply an electrical voltage (approximately 40–50 V) which drives a current through the plate and warms it. The warming process changes the refractive index substantially (to a lesser extent the thickness too) and hence also the distance and position of the interference lines.

The nickel resistor T, which is electrically isolated from the silicon by virtue of a thin silicon nitride layer, used for precise temperature measurement. Due to the extremely small layer thickness the heat is transferred very rapidly from the silicon to the nickel strip with the result that a temperature measurement with a quick response can be presumed. The optical radiation to be filtered enters region A (diameter 6 mm) of the plate. Silicon has the reflection coefficient 0.3 so that the etalon can be used without additional mirrors even if the finesse is relatively small [13]. Finally, the base F plays a decisive role in the etalon functioning since it makes provision for a defined heat dissipation. If the etalon were to be operated in air, the resultant cool-down times would be too long. Glass-fiber-reinforced PTFE is used in the present case and can be deployed up to 250°C. The temperature control is performed by a fast PI controller.

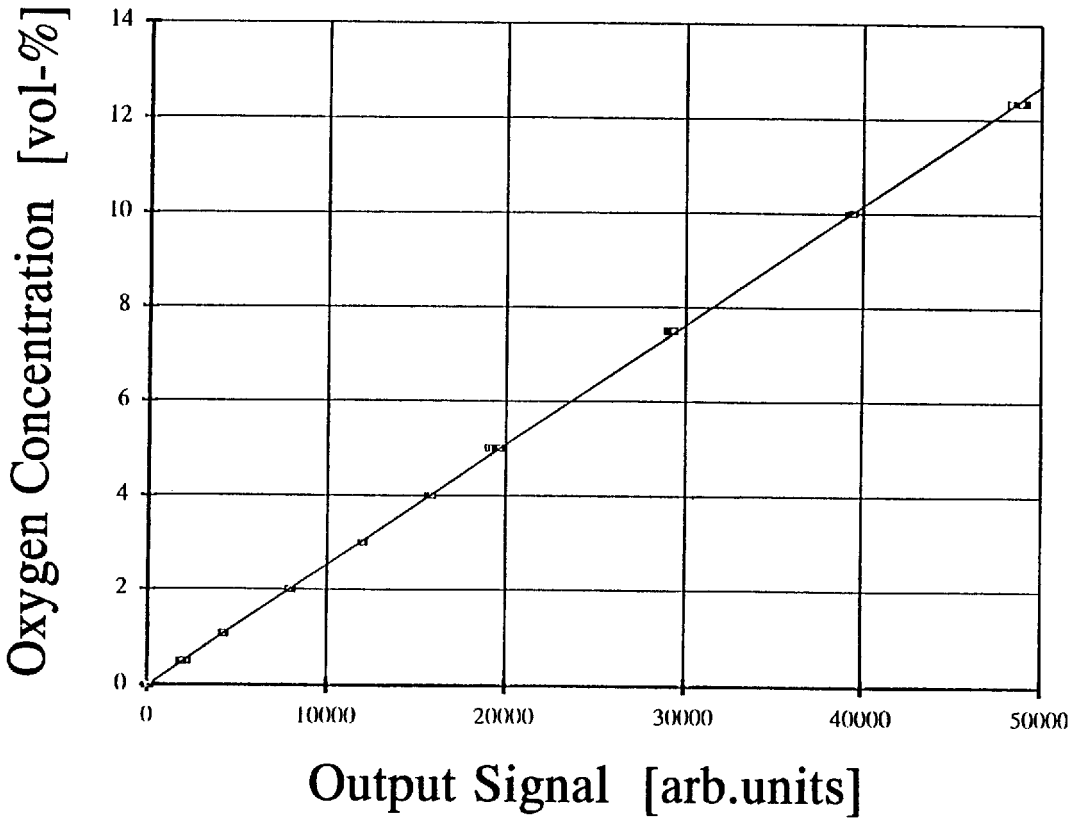

Fig.7. Characteristic of the output signal in the range 0–14 vol-% O2.

Fig.10 illustrates schematically the structure of the entire correlation photometer. The radiation coming from the radiation source (incandescent lamp) is modulated by the chopper and reaches the collimator lense 1. The measuring cell containing the gaseous mixture to be analyzed is situated behind the lense. Then comes the thermally tuned etalon. Using the interference filter, the radiation is restricted to the desired spectral region. The following lense 2 focuses the radiation on a thermoelectrically cooled PbSe detector. A lock-in amplifier, which is not illustrated, attends to phase-sensitive rectification.

During the measurement phase, the etalon temperature is adjusted such that the interference lines coincide exactly with the absorption lines (resonance position). During the reference phase, the interference pattern is displaced by half an interference order (antiresonance position), the measurement and reference radiation thus differ with respect to their spectral fine structure, however, their spectral focal point is identical. Besides both pass through the same optical beam path. If the quotient I_M/I_V is calculated from the time-multiplex detector signals I_M and I_V, corresponding to the measurement and reference phase respectively, a signal is obtained which is independent of the non-specific

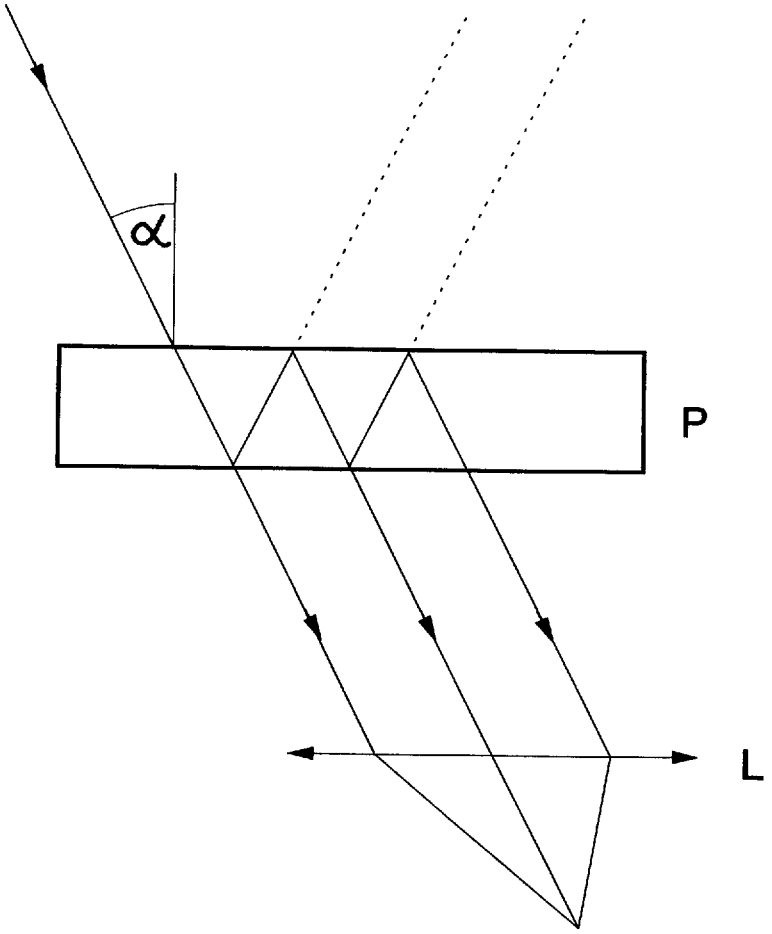

Fig.8. Principle of the etalon, P plate, α angle of incidence, L lens.

fluctuations of the radiant power and of the detector sensitivity. In this manner, the preconditions for high stability of zero and sensitivity are fulfilled.

In the field of medicine technology, the nitrous oxide concentration in the ambient air of the operating theatres is monitored, inter alia. An etalon thickness of approximately 1.5 mm must be selected for this application so that the distance between the interference lines and rotation lines will be equal. Displacement by one order of interference takes place already at a temperature difference of approximately 8°C. The optimal temperature for the measurement and reference phase (difference approx. 4°C) is selected in each case, and the controller is regulated such that the temperature continually fluctuates between these two values. If the etalon is operated at approximately 200°C, the resultant warm-up rate is approximately 25 K/s, and the cool-down rate is approximately 6 K/s. The radiation flux measured in each phase is saved and from it is formed the

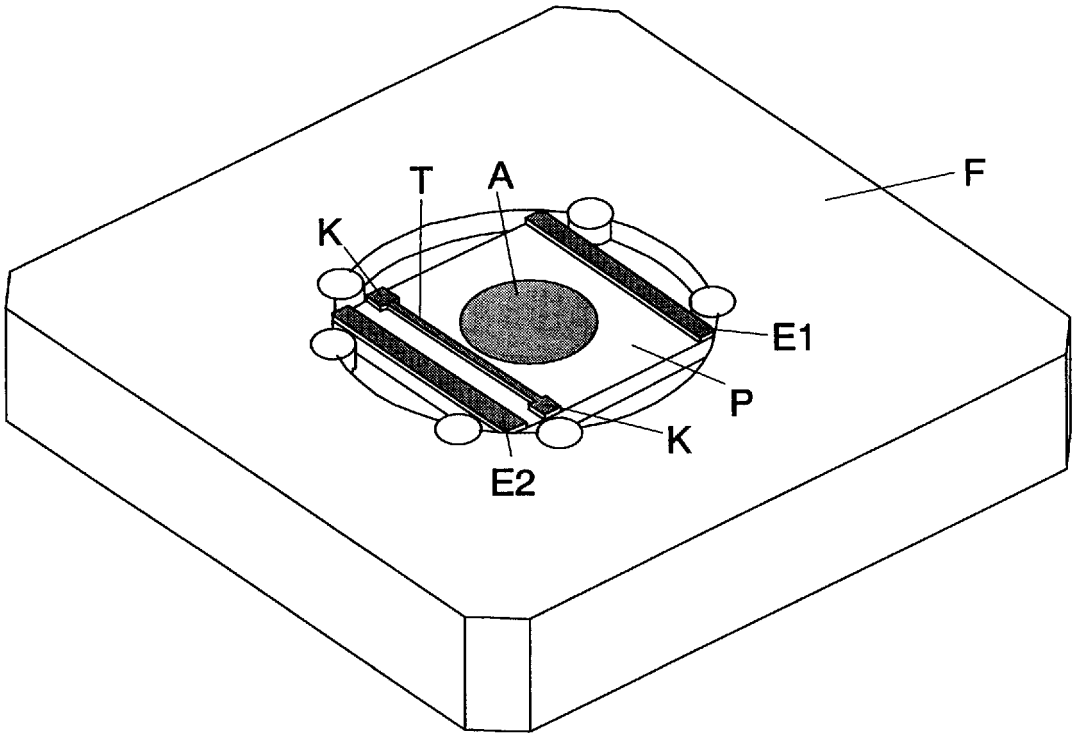

Fig.9. Structure of the silicon etalon. P Silicon plate, $E1$ and $E2$ gold electrodes, T nickel resistor, K electrodes, A aperture, F base.

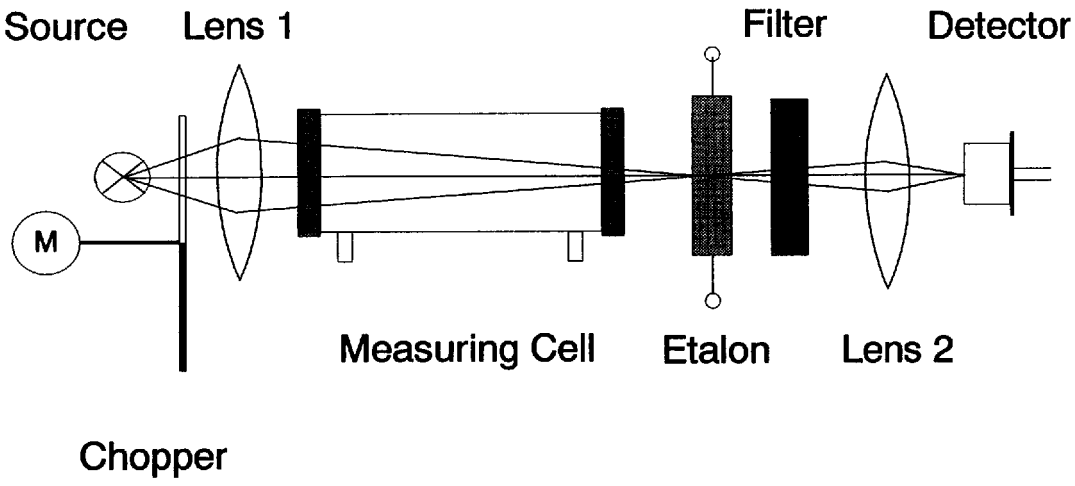

Fig.10. Schematic design of the correlation photometer.

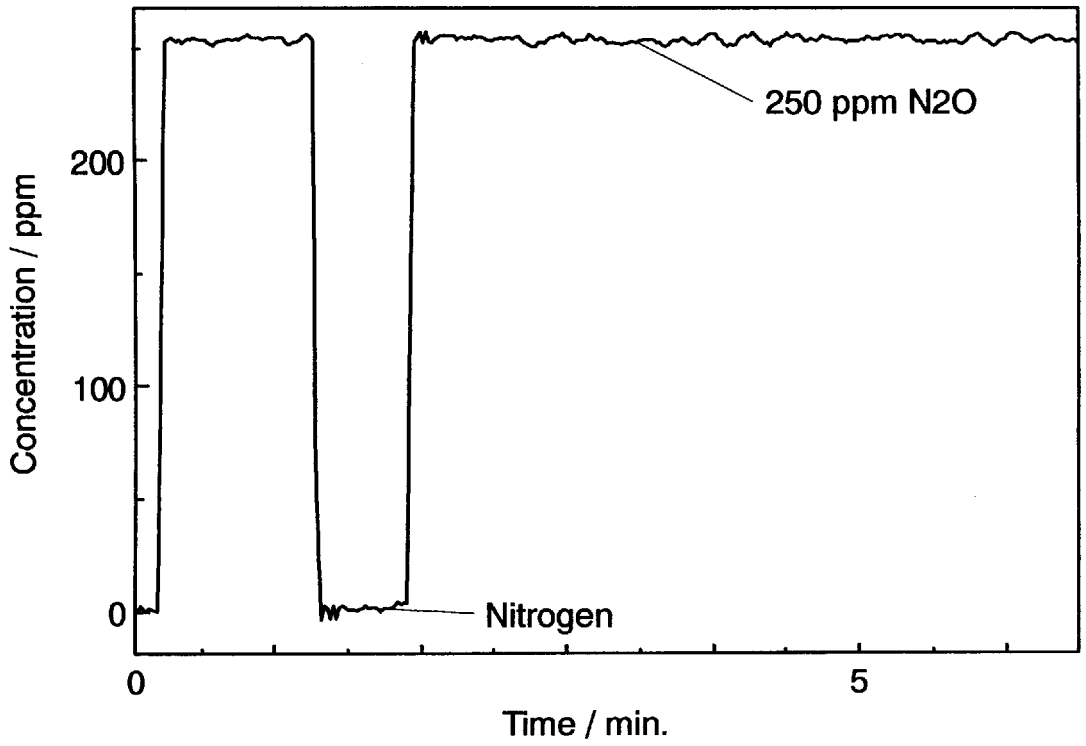

Fig.11. Measurement of the nitrous oxide concentration as a function of time.

time-dependent function which depicts the gas concentration in linear approximation:

$$c(t) = 1 - I_M/I_V. \tag{3}$$

Fig.11 shows such a time-dependent measurement for nitrous oxide. A detection limit of approximately 2 ppm N_2O is inferred from the diagram. The recommended threshold value in operating theatres is 100 ppm; hence N_2O can be safely monitored.

To sum up, the descriptions demonstrate that the Fabry Perot correlation photometer is a high-performance analyzer, with the newly developed tunable silicon etalon making the most important contribution to its success. It has small dimensions, possesses no moveable parts and can be manufactured easily and inexpensively in thin-film technology. The correlation photometer offers interesting deployment possibilities in all areas where other methods run the risk of producing incorrect measurement results due to inadequate selectivity or inadequate stability of zero and sensitivity.

5. Multicomponent FTIR process spectrometer

The FTIR spectrometry (Fourier transform infrared) is a multiplex measuring method where all wavelengths meet simultaneously on a detector (Multiplex or Fellgett advantage [15]). Since there is no need for a slit as in the grating spectrometer, the throughput or Jacquinot advantage is also obtained [15]. The following text describes a

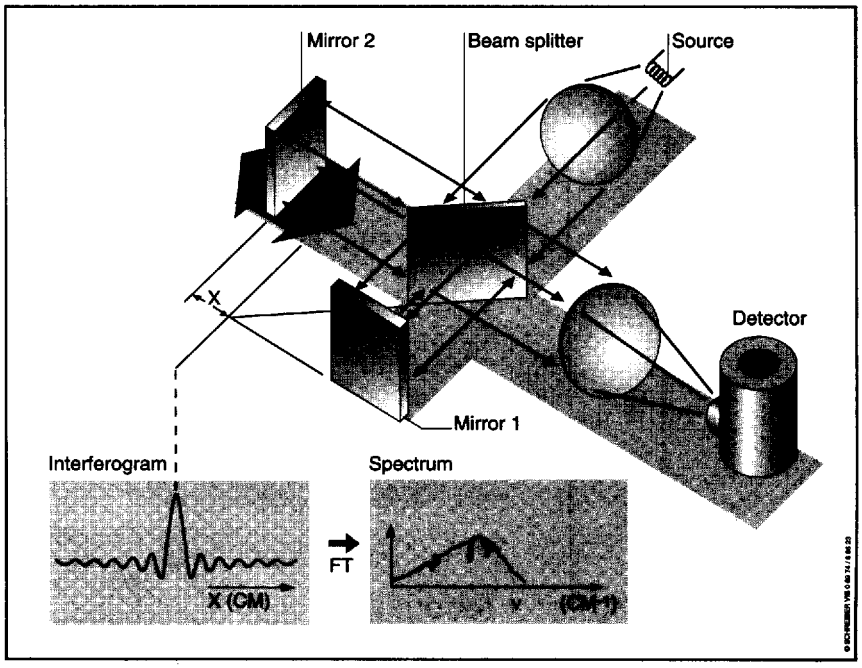

Fig.12. Functional design of a Michelson interferometer.

FTIR spectrometer which, by virtue of its ruggedness and special chemometric software, is particularly suitable for multicomponent process analysis.

The principle FTIR setup is known as Michelson Interferometer and has been dealt with in detail in the specialised literature [15], hence the principle is only cursorily alluded here (Fig.12). The radiation emitted by a broad-band radiation source (e.g. Globar) falls on a beam splitter, which in the most favourable case reflects one half of the incident light and transmits the other half. The reflected half reaches the fixed mirror 1 where it is reflected and again reaches the beam splitter. The other half of the radiation is reflected by mirror 2 which moves to and fro by a certain magnitude X. Finally, both reflected halves interfere at the beam splitter with the path difference $2X$. The resultant radiation passes through the measuring cell, which is not illustrated and reaches the detector. As a function of the path difference X the flow of radiation is registered at the detector as a so-called interferogram. The required radiation spectrum as a function of the wavelength or wavenumber is obtained by Fourier transformation of the interferogram.

Hartmann & Braun/Bomem have developed a particularly rugged version of the Michelson Interferometer [16]. In the so-called wish-bone interferometer (DPI) which is part of the analyzer MB 100 the mirror is not moved linearly but rather tilts to and fro. The DPI has two corner cube mirrors which are mounted on the arms of a rugged right-angled wish-bone swingarm (see Fig.13). The optical path difference between the interferometer arms is produced by movement of the pendulum of the wish-bone swingarm. The spectral resolution of the interferometer is 1 cm^{-1} so that in many cases already the rotational fine structure of the respective gas is visible.

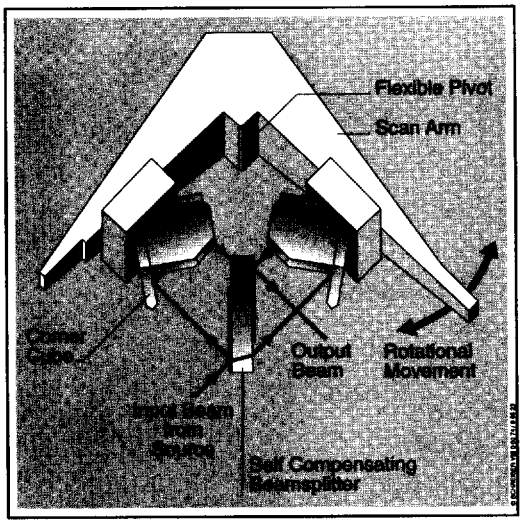

Fig.13. Functional design of the wish-bone swingarm interferometer.

The interferometer MB 100 constitutes the heart of the multicomponent FTIR gas analyzer model 9100 [17], permitting simultaneous emission monitoring of the components SO_2, NO, NO_2, CO, NH_3, CO_2 and HCl in the presence of water vapour (up to 30 vol. %). To obtain a non-falsified measurement of the water-soluble HCl, the same gas must not go below dewpoint temperature from the time of sampling until it reaches the measuring instrument. Hence, the entire gas sampling line including the multireflection cell (6 m effective absorption length) is heated to 180°C. Fig.14 shows a section of a typical absorption spectrum, as is found e.g. in the emission gas of a refuse incineration facility. The most diverse methods have been developed for quantitative evaluation of the absorption spectrum [18]. In this present case, multicomponent software is based on the K-matrix method, which uses the classic least square algorithm [19]. Here the matrix notation for the mathematical approach derived from the Beer's Law:

$$A[m,1] = K[m,n] \cdot C[n,1]. \tag{4}$$

A denotes the absorption vector measured for m wavelength points, K the calibration matrix for m wavelengths and n measured components and C is the concentration vector sought for n measured components. The solution of the equation system acccording to the least square method [19] returns:

$$C[n,1] = (K^T[n,m] \cdot K[m,n])^{-1} \cdot K^T[n,m] \cdot A[m,1]. \tag{5}$$

(T denotes the transposed matrix where lines and columns are interchanged). The equation system is overdetermined, i.e. the number of the wavelength points m evaluated is greater than the number of the measured components n. An important advantage of the K-matrix approach resides in the fact that an additional measured component can be implemented relatively easily in the software. The calibration, which can be easily performed with binary test gases, presents a further advantage.

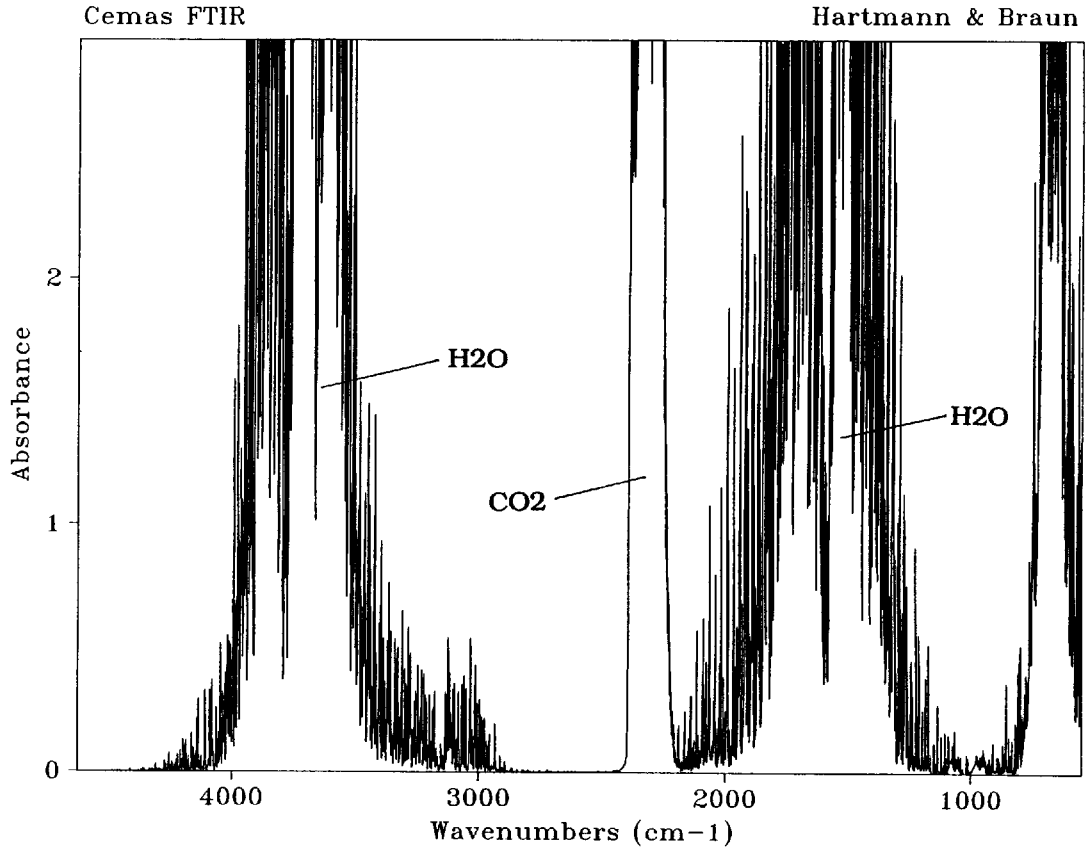

Fig.14. Typical absorption spectrum of the flue gas of a refuse incineration plant.

Fig.15 gives a view of the entire analyzer cabinet while Fig.16 presents a typical form of the measured value representation on the computer display. Measurements conducted so far with the FTIR process spectrometer indicate that the system will establish itself in certain areas of stack gas measurement and also in the chemical industry.

6. Conclusions

The measuring methods described indicate clearly that the spectral selectivity for a required measured component can be realized in the most diverse ways. If one focuses on the obtainable selectivity, the laser bandwidth of approximately 10^{-4} cm^{-1} certainly presents the best value. Using the NDIR and Fabry-Perot correlation method the resolution is "only" of the magnitude of the rotational line width (10^{-1} cm^{-1}). However, due to the correlation across many lines, a comparatively high selectivity can be obtained here [20]. Although the FTIR method reviewed has the lowest resolution 1 cm^{-1}, it nevertheless yields considerable selectivity. The entire infrared spectrum of the gas

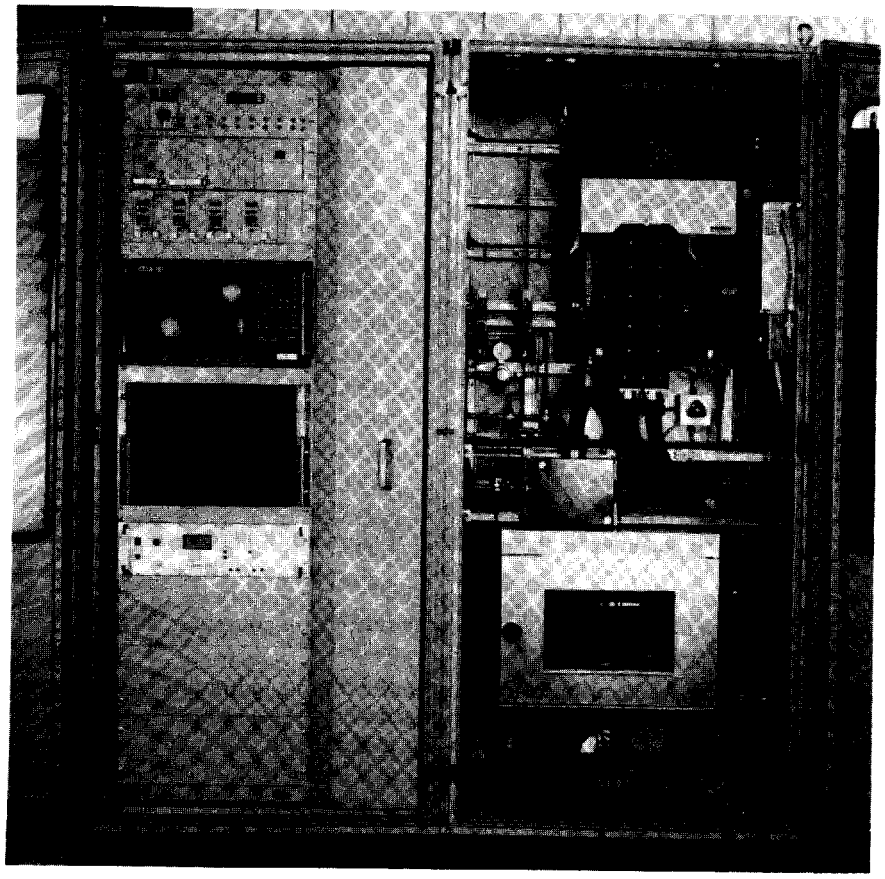

Fig.15. View of the entire analyzer cabinet with FTIR process analyzer.

sample is available here, with the result that there are practically always regions where the measured and interference components do not overlap.

Overall all the measuring methods described have a good chance of establishing themselves on the applications outlined. Due to the advantages presented by the methods described there is every likelihood that new applications will be discovered.

References

[1] M. Zöchbauer; W. Schaefer: Wavelength sensitive detection. Sensors, a comprehensive survey. Vol. 6 Optical sensors, VCH, Weinheim (1982) 277.

[2] W. Schaefer: Die Anwendungen von spektroskopischen Methoden und Lasern zur Bestimmung von gasförmigen Schadstoffen in der Luft. PTB-Mitteilungen 2/74 pp. 84–92 (The applications of spectroscopy methods and lasers for determining gaseous pollutants in the air.)

[3] K. F. Luft; W. Schaefer; G. Wiegleb: 50 Jahre NDIR-Gasanalyse. (50 years of NDIR gas analysis). Technisches Messen 60 (1993) 363.

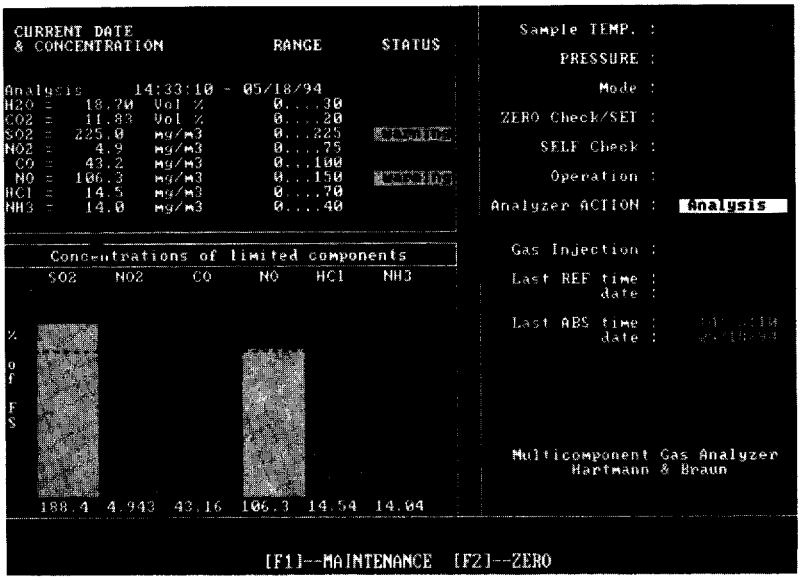

Fig.16. View of the measured value output on computer display.

[4] G. Kesseler: Über die Absorption von ultraroter Strahlung in hintereinanderliegenden Gasschichten und ihre Bedeutung für photometrische Analysenverfahren. (On the absorption of ultrared radiation on gas layers placed one behind the other and on their significance for photometric analytic methods.) Dissertation TU-Clausthal (1967).

[5] M. Phillips: Breath Test in Medicine. Scientific American July (1992) 52.

[6] E. Löbach: 13C-Harnstoff-Atemtest nach dem CEDIOX-Verfahren. Mitteilung der TOPIC AG Liechtenstein. (Urea Breadth Test acc. to CEDIOX Method. Report of TOPIC AG Liechtenstein).

[7] W. Fabinski; G. Wiegleb; P. Hering; W. Fuss; M. Haisch: Europäische Patentanmeldung No.: 93250208.1 (1993) (European Patent Application No.: 93250208,1 (1993)).

[8] E. D. Hinkley: Laser Monitoring of the Atmosphere. Topics in Applied Physics Vol. 14; Berlin, Heidelberg, New York, Tokio: Springer Verlag, 1976.

[9] H. Kildal; R. L. Byer: Comparison of Laser Methods for the Remote Detection of Atmosphere Pollutants. Proc. IEEE 59 (1971) 1644.

[10] V. Ebert; J. Wolfrum: Internal Report of the Institute of Physical Chemistry (University of Heidelberg) 1994.

[11] G. Fortunato; A. Marechal; M. Wolfer: Application of interferential correlation of spectra to the detection of pollutants in the atmosphere. SPIE Proc. Vol. 136 (1977) 14.

[12] J. P. Dakin; C. A. Wade; D. Pinchbeck; J. S. Wykes: A novel optical fibre methane sennsor. Proc. Int. Conf. Fibre Optics '87, London. SPIE Proc. Vol. 734 (1987), Paper 33.

[13] M. Zöchbauer: Entwicklung eines thermisch abstimmbaren Fabry-Perot-Korrelationsspektrometers für die Gasanalyse. (Development of a thermally adjustable Fabry-Perot Correlation Spectrometer for Gas Analysis). Dissertation, Johann Wolfgang Goethe-Universität Frankfurt/M. 1993.

[14] W. Füller; B. Horn; Th. Liedtke; M. Moede; M. Zöchbauer: Deutsches Patent P4119461 (German Patent P4119461).

[15] P. R. Griffiths; J. A. de Haseth: Fourier transform infrared spectrometry. New York: John Wiley and Sons, 1986.

[16] R. G. Jaacks; HH. Rippel: Appl. Optics 1 (1989) 29.

[17] A. Rilling; D. Gravel; S. Perry; M. Baillargeon; A. Chambrland: An FT-IR based CEMS (Continuous emissions monitoring system). Municipal waste combustion conference, March 30–April 6, 1993, Virginia.

[18] K. R. Beebe; B. R. Kowalski: An introduction to multivariate calibration and analysis. Anal. Chem. 59 (1987) 1007.

[19] D. M. Haaland; R. G. Easterling; D. A. Vopicka: Multivariate least-squares methods applied to the quantitative spectral analysis of multicomponent samples. Appl. Spectr. 39 (1985) 73.

[20] A. Galais; G. Fortunato; P. Chavel: Gas concentration measurement by spectral correlation: rejection of interferent species. Appl. Optics 24 (1985) 2127.